buildings

MDPI

*Article*

# Investigation of Intermediate-Height Horizontal Brace Forces under Horizontal and Vertical Loads including Random Initial Imperfections

**Haixu Yang [1,*], Shuo Liu [1], Zhiyuan Fang [2,3,*] and Jinyou Zhao [1,4,*]**

1 School of Civil Engineering, Northeast Forestry University, Harbin 150040, China
2 School of Engineering, The University of Waikato, Hamilton 3240, New Zealand
3 Department of Civil and Environmental Engineering, The University of Auckland, Auckland 1023, New Zealand
4 School of Urban Construction and Safety Engineering, Shanghai Institute of Technology, Shanghai 201418, China
* Correspondence: yhxcumt@163.com (H.Y.); afang@waikato.ac.nz (Z.F.); jinyou2000@sit.edu.cn (J.Z.)

**Abstract:** In engineering practice, longitudinal brace systems for column-braced systems are designed to resist both horizontal and vertical loads. In previous experimental research on horizontal brace forces for column-braced systems of intermediate height, only vertical loads were considered. Hence, this paper presents a numerical simulation of numerous column-braced systems subjected to horizontal and vertical loads. In the numerical simulation, second-order analysis was adopted, and the Monte Carlo method was used to incorporate the randomness of initial imperfections in the horizontal brace and column. From the finite element (FE) analyses and probability model statistics, the normal probability density equation for intermediate-height horizontal brace forces under horizontal and vertical loads was obtained, and the corresponding design intermediate-height horizontal brace forces were determined and compared with those under vertical loads only. The results indicate that the design intermediate-height horizontal brace forces under horizontal and vertical loads are significantly greater than those under only vertical loads, and that the design intermediate-height horizontal brace forces under horizontal and vertical loads are also greater than the simple superposition results of horizontal loads and intermediate-height horizontal brace forces under only vertical loads.

**Keywords:** intermediate-height horizontal brace forces; horizontal loads; vertical loads; Monte Carlo method; random initial imperfection; probability statistics

check for updates

**Citation:** Yang, H.; Liu, S.; Fang, Z.; Zhao, J. Investigation of Intermediate-Height Horizontal Brace Forces under Horizontal and Vertical Loads including Random Initial Imperfections. *Buildings* **2023**, *13*, 180. https://doi.org/10.3390/buildings13010180

Academic Editor: Charalampos Baniotopoulos

Received: 22 November 2022
Revised: 4 January 2023
Accepted: 9 January 2023
Published: 9 January 2023



## 1. Introduction

The role of braces has been well understood in practical engineering [1]. Bracing members in structural systems were divided into two categories according to the roles of braces: one resisting horizontal loads, including wind loads, earthquake loads, and crane loads, and the other providing intermediate lateral support to the member's weak axis for enhancing its stability [2]. To reduce effective column lengths and resist longitudinal horizontal loads under vertical loads, the longitudinal bracing systems of column-braced systems of industrial plants are commonly composed of horizontal braces and diagonal braces. In practical engineering, the structure will bear vertical and horizontal loads, in which the horizontal load includes wind loads, earthquake loads, and crane loads besides providing support for structural stability. The design intermediate-height horizontal brace forces in column-braced systems under vertical loads have generally been investigated [3–6], but no important definitive research has been conducted on the design intermediate-height horizontal brace forces in column-braced systems under horizontal and vertical loads.

In previous studies on column-braced systems subject to vertical loads [5–9], the Monte Carlo method accounted for the randomness of initial imperfections in the horizontal brace and column. Research results have shown that the random combination of initial imperfections between the columns and horizontal braces has a positive effect on brace forces as it leads to the randomness of the intermediate-height horizontal brace forces in compression or in tension when the ultimate load of the braced columns is reached. Thus, to ensure the accuracy of intermediate-height horizontal brace forces under horizontal and vertical loads, it is necessary to account for the effects of initial imperfections [8–15].

In this study, a second-order analysis of extended column-braced systems under horizontal and vertical stresses was conducted using the ANSYS program [16] and the Monte Carlo method to randomly sample the initial imperfections of horizontal braces and column. Furthermore, the normal probability density equation of the intermediate-height horizontal brace forces under horizontal and vertical loads was proposed on the basis of the probability statistics method, and the design intermediate-height horizontal brace forces were also proposed and compared with those under only vertical loads.

## 2. Parametric Design and Analytical Model

The purpose of this paper is to only study the longitudinal brace force of the horizontal brace, because the longitudinal direction is about the weak axis of the column and will cause overall instability. The transverse frame was not considered, because it is about the strong axis of the column and will not cause overall instability. Therefore, the planar scheme was chosen. The analytical model validated by Ref. [17] was adopted in this paper. Finite element (FE) analysis results and test results are summarized in Table 1. Instability deformations obtained from the tests and FE analyses are shown in Figures 1 and 2. In terms of the ultimate loads and instability deformations, the FE analysis results showed good agreement with test results. Therefore, it can be considered that the FE analysis model could accurately simulate the test.

**Table 1.** Test results and FE analysis results.

| Test | Test Results | | | FE Analysis Results | | | $P_{uf}/P_{ut}$ | $F_{uf}/F_{ut}$ |
|---|---|---|---|---|---|---|---|---|
| | Ultimate Loads $P_{ut}$ /N | Maximum Horizontal Brace Force $F_{ut}$/N | $F_{ut}/P_{ut}$ | Ultimate Loads $P_{ut}$ /N | Maximum Horizontal Brace Force $F_{ut}$/N | $F_{ut}/P_{ut}$ | | |
| Group 1 | 7616 | 492 | 0.065 | 8145 | 617 | 0.076 | 1.07 | 1.25 |
| Group 2 | 7121 | −484 | −0.068 | 7830 | −609 | −0.078 | 1.11 | 1.26 |

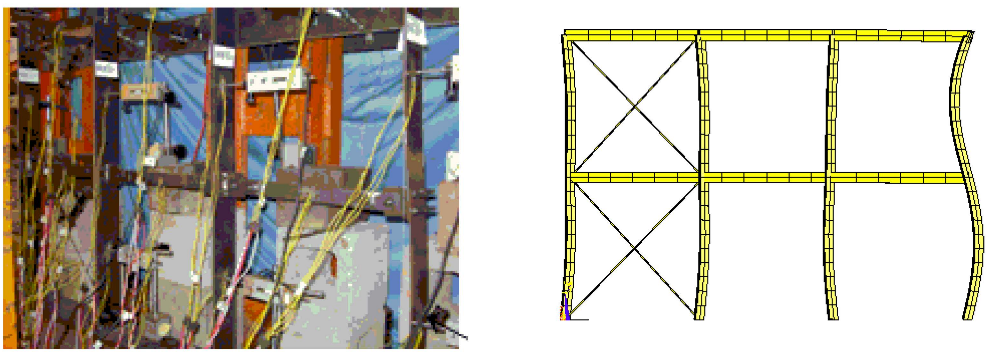

(**a**) (**b**)

**Figure 1.** Instability deformation obtained from the tests and FE analyses of Group 1. (**a**) Tests; (**b**) FE analyses.

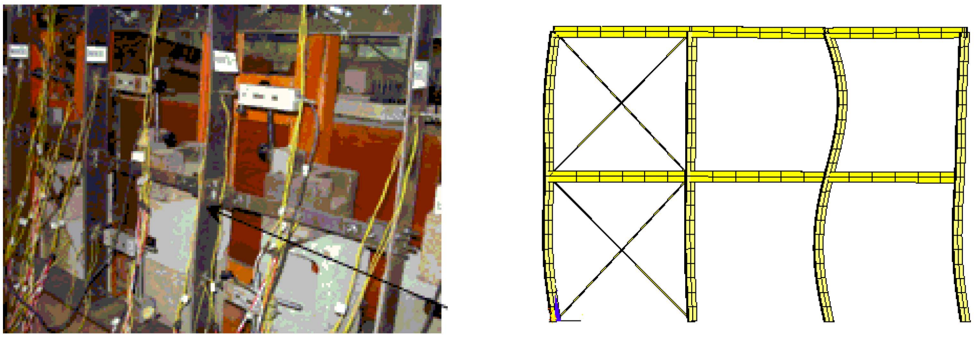

(**a**) (**b**)

**Figure 2.** Instability deformation obtained from the tests and FE analyses of Group 2. (**a**) Tests; (**b**) FE analyses.

The analytical models for column-braced systems under horizontal and vertical loads are shown in Figure 3. The identical vertical axial load $P$ was applied to simply supported $n$-columns with equal spacing, and the horizontal loads of the left and right ends at the top of the braced columns are $H_1 = \gamma_1 P$ and $H_2 = \gamma_2 P$, respectively. $\gamma_1$ and $\gamma_2$ are the horizontal load coefficients of the left and right ends at the top of the braced columns, respectively. $A_c$ represents the sectional areas of each column.

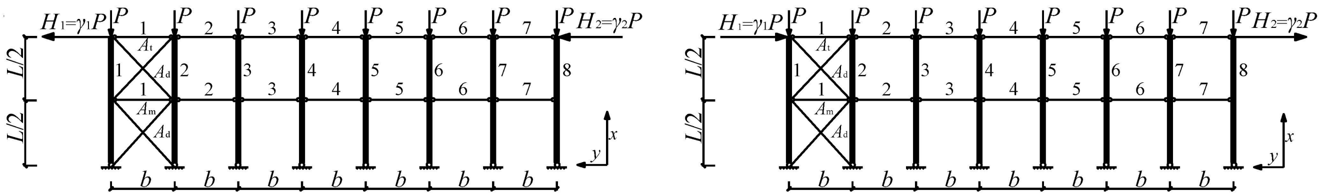


(**a**) (**b**)

**Figure 3.** Analytical models of column-braced systems under horizontal and vertical loads. (**a**) The horizontal loads to the left; (**b**) The horizontal loads to the right.

For the analytical models, the parameter selection was mainly based on Ref. [6]. It should be noted that only vertical loads were considered in the previous study [6]. In most practical engineering, the following parameters are commonly used: the slenderness ratio of the horizontal brace ($100 \leq \lambda_b \leq 200$); the horizontal brace length ($b$ = 6 m); and the ratio of horizontal brace length to column height, ($0.4 \leq b/L \leq 0.7$). According to Ref. [6], the half slenderness ratio ($\lambda_c$ = 100) of the column about the weak axis is conservatively adopted in this study. According to the limitations of the above conditions, the dimensions of columns and braces could not adopt normalized profiles. An I-section with biaxially symmetry was selected as the section of the column, whose sectional area is 250 cm$^2$, as shown in Table 2. Flexural buckling on the weak axis of the column occurs in the longitudinal direction of column-braced systems.

**Table 2.** Detailed sectional dimensions of the column.

| $b/L$ | $L$ (m) | $H$ (mm) | $t_w$ (mm) | $B$ (mm) | $t_f$ (mm) | $A_d$ (cm$^2$) |
|---|---|---|---|---|---|---|
| 0.4 | 15 | 800 | 15 | 352.54 | 19.26 | 14.0 |
| 0.5 | 12 | 800 | 17 | 298.81 | 20.22 | 12.0 |
| 0.6 | 10 | 800 | 18 | 256.49 | 22.22 | 11.2 |
| 0.7 | 8.57 | 800 | 19 | 226.98 | 23.56 | 10.5 |

Note: $H$ represents the height of the I-section; $B$ represents the width of the I-section; $t_w$ represents the thickness of the web; $t_f$ represents the thickness of the flange; $A_d$ represents the sectional areas of each diagonal brace.

A circular tube section was selected as the section of the horizontal brace. According to the number of columns, the sectional areas of the horizontal braces were determined. Table 3 lists the detailed sectional dimensions of the horizontal braces where $n$ is equal to 6.

**Table 3.** Detailed sectional dimensions of the horizontal brace.

| $\lambda_b$ | $A_i$ /$A_t$ (cm$^2$) | $D_b$ (mm) | $t_b$ (mm) |
|---|---|---|---|
| 100 | 24 | 169.65 | 4.50 |
| 125 | 32 | 135.56 | 7.51 |
| 150 | 42 | 112.51 | 11.88 |
| 175 | 53 | 95.35 | 17.69 |
| 200 | 64 | 81.01 | 25.14 |

Note: $A_i$ represents the sectional areas of the intermediate height of each horizontal brace; $A_t$ represents the sectional areas of the top of each horizontal brace; $D_b$ represents the external diameter of the circular tube section; $t_b$ represents the thickness of the circular tube section.

A circular solid bar was selected as the diagonal brace, whose sectional areas are listed in Table 2 when $n$ is equal to 6.

## 3. Random Combination of Initial Imperfections

### *3.1. The Monte Carlo Method*

By employing FE analysis and probability model statistics, the Monte Carlo method [18] is capable of solving complex random engineering issues. Using random sampling of small sample sizes, the Monte Carlo method can tackle the large-sample problem. As long as a sufficient sample sum is sampled and simulation tests are reliable, the Monte Carlo method yields credible results [19].

### *3.2. Probability Model of Initial Imperfections*

On the basis of the Monte Carlo method, a normal distribution can be used to represent each random variable [20]. Assuming that $n$ represents the number of columns and $\delta_{0i}$ represents the $i$th column's initial bow imperfection, its probability model distribution is expressed by the following equation.

$$P_i(\delta_{0i}) = \frac{1}{\sqrt{2\pi}\sigma_1} e^{-\frac{(\delta_{0i}-\mu_1)^2}{2\sigma_1{}^2}} \quad i = 1, 2, \ldots\ldots, n \tag{1}$$

Assuming that $\Delta_{0i}$ represents the initial sway imperfection of the $i$th column, its probability model distribution is expressed by the following equation.

$$P_i(\Delta_{0i}) = \frac{1}{\sqrt{2\pi}\sigma_2} e^{-\frac{(\Delta_{0i}-\mu_2)^2}{2\sigma_2{}^2}} \quad i = 1, 2, \ldots\ldots, n \tag{2}$$

Assuming that $u_{0i}$ represents the initial imperfection of the $i$th intermediate-height horizontal brace, its probability model distribution is expressed by the following equation.

$$P_i(u_{0i}) = \frac{1}{\sqrt{2\pi}\sigma_3} e^{-\frac{(u_{0i}-\mu_3)^2}{2\sigma_3{}^2}} \quad i = 1, 2, \ldots\ldots, n-1 \tag{3}$$

Assuming that $v_{0i}$ represents the initial imperfection of the $i$th top horizontal brace, its probability model distribution is expressed by the following equation.

$$P_i(v_{0i}) = \frac{1}{\sqrt{2\pi}\sigma_4} e^{-\frac{(v_{0i}-\mu_4)^2}{2\sigma_4{}^2}} \quad i = 1, 2, \ldots\ldots, n-1 \tag{4}$$

where the mean value $\mu_1 = \mu_2 = \mu_3 = \mu_4 = 0$ and the mean square deviation $\sigma_1{}^2 = \sigma_2{}^2 = L/980$ and $\sigma_3{}^2 = \sigma_4{}^2 = b/980$ [21]. The meaning of initial bow and sway imperfection are shown in Figure 4.

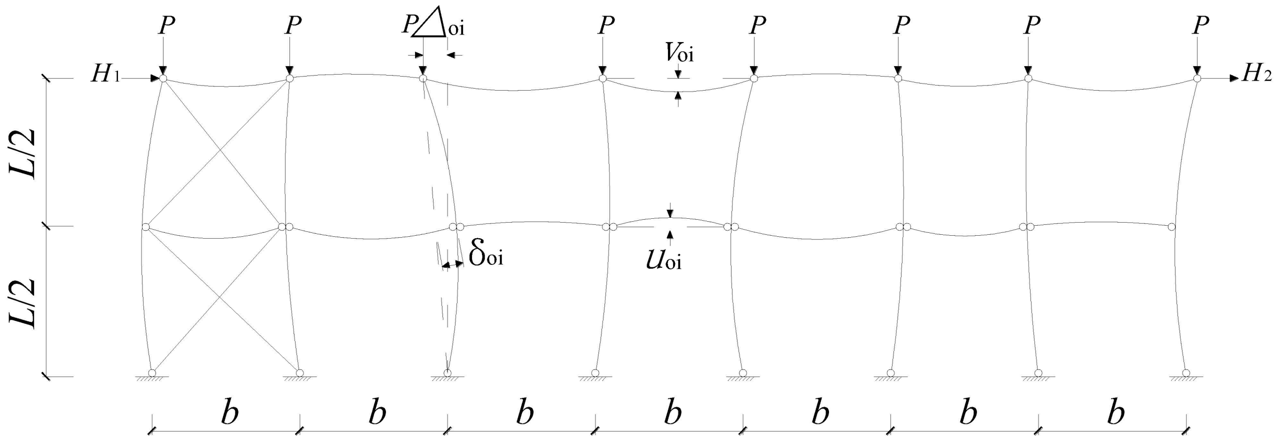


**Figure 4.** The initial bow and sway imperfection of the column, the initial imperfection of the intermediate-height horizontal brace, and the initial imperfection of the *i*th top horizontal brace.

### *3.3. Equations for Random Initial Imperfection*

The *i*th column's initial bow imperfection is given as follows.

$$\delta_i = \delta_{0i} \sin(\frac{\pi x}{L}) \tag{5}$$

The *i*th column's initial sway imperfection is expressed as follows.

$$\Delta_i = \Delta_{0i} \left(\frac{x}{L}\right) \tag{6}$$

The *i*th horizontal brace's initial bow imperfection at the intermediate height of the column is displayed as follows.

$$u_i = u_{0i} \sin(\frac{\pi y}{b}) \tag{7}$$

The *i*th horizontal brace's initial bow imperfection at the top of the column is shown as follows.

$$v_i = v_{0i} \sin(\frac{\pi y}{b}) \tag{8}$$

where $\delta_{0\mathrm{i}}$ represents the initial bow imperfections of the *i*th column; $\Delta_{0\mathrm{i}}$ is the initial sway imperfection of the *i*th column; $u_{0\mathrm{i}}$ represents the initial bow imperfections of the *i*th horizontal brace at the intermediate height of the column; and $\nu_{0i}$ represents the initial bow imperfections of the *i*th horizontal brace at the top of the column. The above parameters were sampled applying the Monte Carlo method.

## 4. Numerical Analysis by the Monte Carlo Method

### *4.1. Numerical Model*

In the ANSYS program [16], the Beam 188 element was used to simulate columns and horizontal braces, while the Link10 element was utilized to simulate the diagonal braces. The hinged joints were simulated at the nodes of horizontal braces and columns by coupling translational displacements. There were twelve elements for each column member, six elements for each horizontal brace member and only one element for each diagonal brace member. According to Equations (5)–(8), the coordinates including the initial imperfections' magnitudes and the directions were built up for these elements [22–26].

### *4.2. Random Sampling of Initial Imperfections*

According to GB 50205-2001 [27], the allowable manufacturing variations for columns in one-story steel buildings are as follows: the maximum initial bow imperfection is 1/1200 of the column's length, whereas the maximum initial sway imperfection is

1/1000 of the column's length. The maximum allowable manufacturing deviations for horizontal braces are 1/750 of the horizontal brace length.

The function 'Normrnd()' in the MATLAB program was used to randomly sample both horizontal and vertical initial imperfections based on their mean and variance. In this paper, 1.05 times the permissible manufacturing variation in GB 50205-2001 was regarded as a sample constraint for initial imperfections, and all samples' initial imperfections had to be be fewer than the sample restrictions [28].

### *4.3. Numerical Analysis*

A bilinear elastic–plastic constitutive relationship model was established for FE analysis. G235 steel was considered as the research objective. The arch-length method was used for non-linear large displacement analysis, in which the maximum loads of the column-braced systems were obtained and served as the strengths of columns [29].

The column-braced systems including the initial imperfections with randomness under horizontal and vertical loads were modeled. When $n$ and horizontal load combination ($H_1 = \gamma_1 P$ and $H_2 = \gamma_2 P$, see Figure 3) are certain, the values $b/L$ and $\lambda_b$ exist in twenty combinations. For the initial imperfections of both horizontal braces and columns, a total of 50 groups of random samples were taken from each combination, giving each specific constitution a total of one thousand random combinations. The findings of the investigation revealed that both the columns and horizontal braces were extremely sensitive to the initial imperfections' direction and magnitude.

## 5. Effect of Horizontal Load Combinations on Intermediate-height Horizontal Brace Forces

### *5.1. Probability Density Figures of F/P under Different Horizontal Load Combinations*

Taking column number $n = 8$ and the horizontal load coefficient $\gamma = 0.02$ as examples, three kinds of horizontal load combinations ($\gamma_1 = 0$ and $\gamma_2 = \gamma$, $\gamma_1 = \gamma/2$ and $\gamma_2 = \gamma/2$, $\gamma_1 = \gamma$ and $\gamma_2 = 0$) were considered when the horizontal load was to the left or right, as shown in Figure 3. As shown in Figure 5, two kinds of sway instability deformation modes could be obtained for column-braced systems under horizontal and vertical loads, respectively, in which the maximum intermediate-height horizontal brace force was subjected to compression.

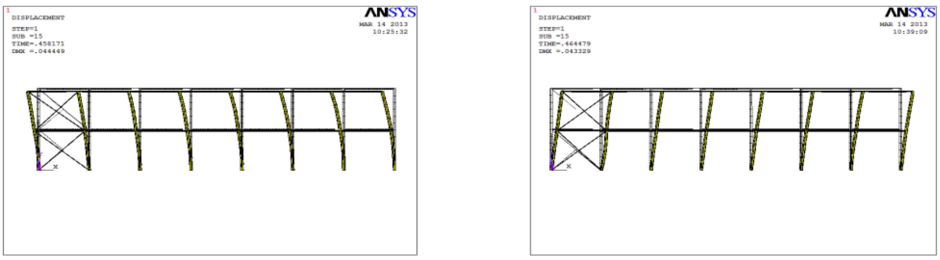

(**a**) (**b**)

**Figure 5.** Instability modes of column-braced systems under horizontal and vertical loads. (**a**) The horizontal loads to the left; (**b**) The horizontal loads to the right.

A total of six groups of $F/P$ ratios were determined by considering three types of horizontal load combinations and two horizontal load directions (left and right). $F$ refers to maximum intermediate-height horizontal brace force, and $P$ refers to the column ultimate load. As noticed previously, for each certain constitution between $n$ and the horizontal load combination, a total of one thousand FE analysis results are significantly influenced by $\lambda_b$, $b/L$, and the initial imperfection with randomness in the horizontal braces and columns. Obviously, due to the initial imperfections with randomness in the horizontal braces and columns, the FE analysis results of $F/P$ are also random. The probability statistics method was used to analyze the FE analysis results.

The results of six groups of $F/P$ ratios obtained from different horizontal load combinations are presented in Figure 6. The relative frequencies were taken as the ordinates for various values of $(F/P) \times 100$ (the abscissa). The probability of each abscissa value obtained from the FE analysis is represented by the area of single blue rectangle, and the sum of all the rectangular areas is 1. The theoretical probability density equations for the normal distributions represented by the solid lines were selected to fit the data.

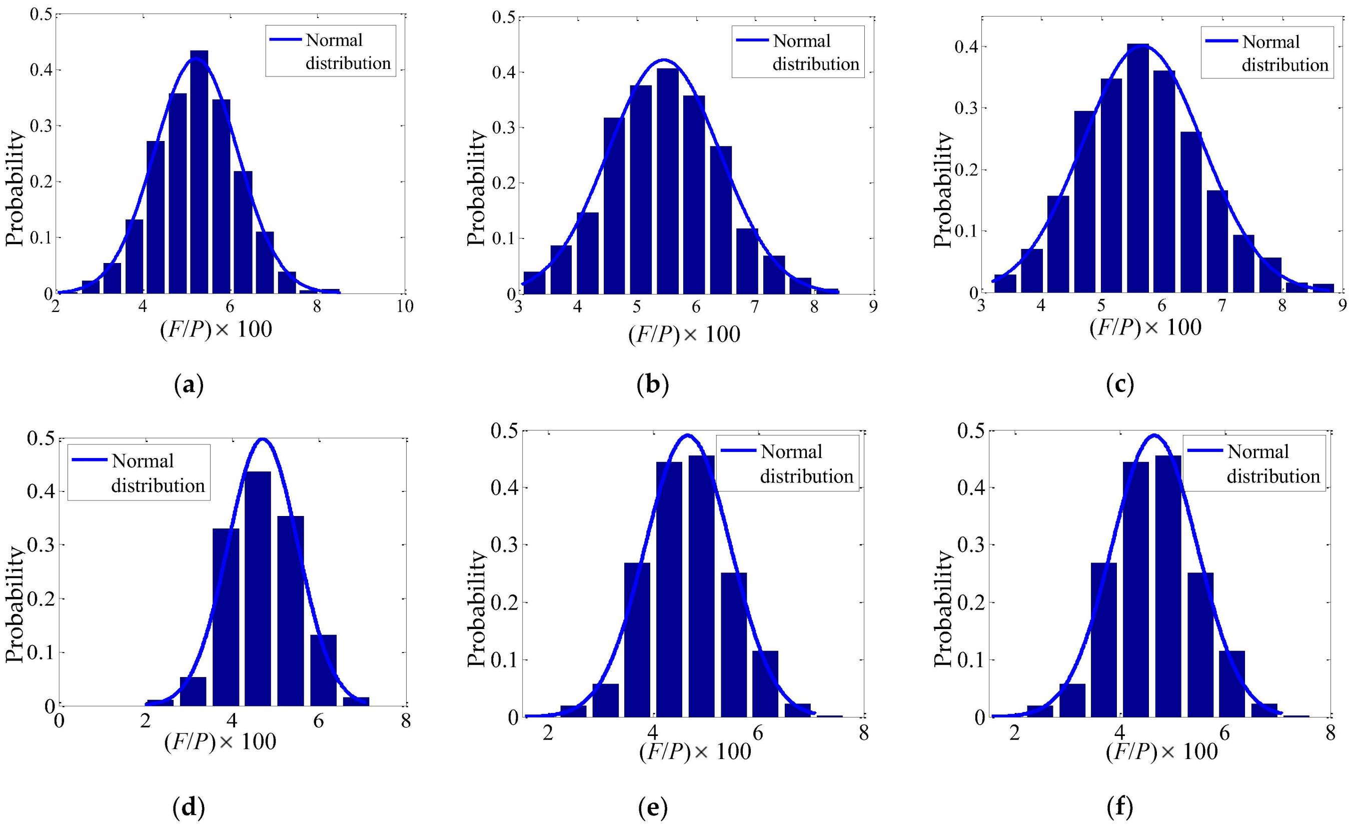


**Figure 6.** Probability density figures of $F/P$ under different horizontal load combinations. (**a**) The left horizontal loads with $\gamma_1 = \gamma$ and $\gamma_2 = 0$; (**b**) The left horizontal loads with $\gamma_1 = \gamma/2$ and $\gamma_2 = \gamma/2$; (**c**) The left horizontal loads with $\gamma_1 = 0$ and $\gamma_2 = \gamma$; (**d**) The right horizontal loads with $\gamma_1 = \gamma$ and $\gamma_2 = 0$; (**e**) The right horizontal loads with $\gamma_1 = \gamma/2$ and $\gamma_2 = \gamma/2$; (**f**) The right horizontal loads with $\gamma_1 = 0$ and $\gamma_2 = \gamma$.

### *5.2. Normal Distribution of F/P*

The normal probability density equation for $F/P$ is expressed as follows.

$$f(x) = \frac{1}{\sqrt{2\pi}\sigma} \exp\left[-\frac{1}{2}\left(\frac{x-\mu}{\sigma}\right)^2\right] \tag{9}$$

The distribution equation for $F/P$ is expressed as follows.

$$F(x) = \frac{1}{\sqrt{2\pi}\sigma} \int_{-\infty}^{x} e^{-\frac{1}{2}\left(\frac{t-\mu}{\sigma}\right)^2} dt \tag{10}$$

where $\sigma$ is the mean-square deviation and $\mu$ is the average value for the one thousand $(F/P) \times 100$ numerical results. $F$ refers to the maximum intermediate-height horizontal brace force, and $P$ refers to the column ultimate load. The statistical results for various values of $(F/P) \times 100$ under different horizontal load combinations are displayed in Table 4.

**Table 4.** Statistical results of $(F/P) \times 100$ and $F_n/P$ * under different horizontal load combinations.

| $n$ | Direction of the Horizontal Loads | Different Horizontal Load Combinations ($\gamma$ = 0.02) | Statistical Character | $F_n/P$ | $1.2 \times F_n/P$ |
|---|---|---|---|---|---|
| 8 | To the left | $\gamma_1 = 0, \gamma_2 = \gamma$ | $\mu = 5.6789; \sigma = 0.9944$ | 7.31% | 8.77% |
| | | $\gamma_1 = \gamma/2, \gamma_2 = \gamma/2$ | $\mu = 5.4559; \sigma = 0.9468$ | 7.01% | 8.41% |
| | | $\gamma_1 = \gamma, \gamma_2 = 0$ | $\mu = 5.2668; \sigma = 0.9556$ | 6.78% | 8.14% |
| | To the right | $\gamma_1 = 0, \gamma_2 = \gamma$ | $\mu = 4.7061; \sigma = 0.8022$ | 6.01% | 7.21% |
| | | $\gamma_1 = \gamma/2, \gamma_2 = \gamma/2$ | $\mu = 4.6539; \sigma = 0.8139$ | 5.98% | 7.18% |
| | | $\gamma_1 = \gamma, \gamma_2 = 0$ | $\mu = 4.6083; \sigma = 0.8308$ | 5.96% | 7.15% |

* $F_n/P$: See Figure 7 for the characteristic value $F_n/P$.

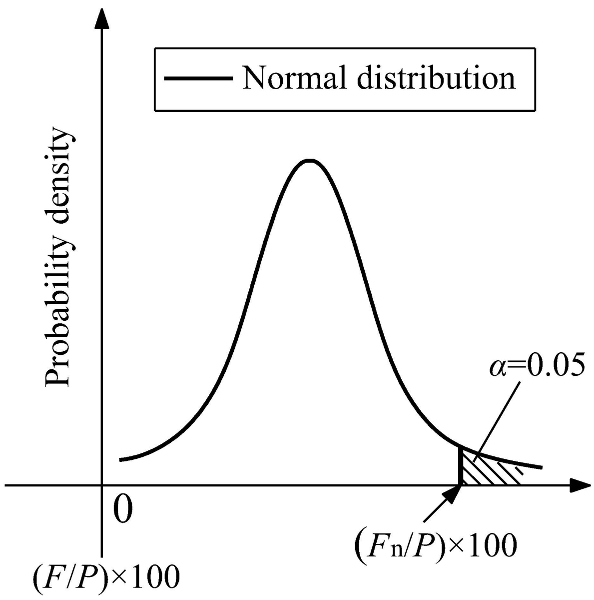


**Figure 7.** The characteristic values at $\alpha$ = 0.05.

### *5.3. Design Intermediate-height Horizontal Braces Forces*

As mentioned previously, the distribution equations $F(x)$ can predict the $F/P$ ratio to a certain significance level, $\alpha$. In this paper, $\alpha$ = 0.05 was selected as the significance level and then the characteristic values $F_n/P$ were selected as the force of an intermediate-height horizontal brace with a 95% guarantee rate, as displayed in Figure 7.

$F_n/P$ needs to be multiplied by a coefficient of 1.2 to give more support for longitudinal columns, and is selected as the design intermediate-height horizontal brace force. The values for $1.2 \times F_n/P$ and $F_n/P$ under different horizontal load combinations are summarized in Table 4.

### *5.4. The Most Unfavorable Horizontal Load Combination*

Table 4 shows a comparison of the design intermediate-height horizontal brace forces $1.2 \times F_n/P$ under different horizontal load combinations. It can be seen that $1.2 \times F_n/P$ under the left horizontal loads is higher than that under the right horizontal loads, and that $1.2 \times F_n/P$ is the maximum when the left horizontal loads act fully at the right top of the braced columns, i.e., $\gamma_1 = 0$ and $\gamma_2 = \gamma$. The above phenomenon may be related to the direction and position of the horizontal loads. When the horizontal loads are to the left, the intermediate-height horizontal brace force is in the same direction as the left horizontal load, which can increase the intermediate-height horizontal brace force. When the horizontal loads are away from the diagonal braces, the diagonal braces will resist less horizontal load, which can result in higher intermediate-height horizontal brace forces [30].

## 6. Intermediate-height Horizontal Brace Forces under the Most Unfavorable Horizontal Load Combination

### 6.1. Probability Density Figures of F/P under the Most Unfavorable Horizontal Load Combination

As noted before, it is most unfavorable for the intermediate-height horizontal brace force when the left horizontal loads act entirely at the right top of the columns; therefore, Figure 8 depicts the analytical model for a column-braced system under the most unfavorable horizontal load combination. A total of 20 sets of column-braced systems under the most unfavorable horizontal load combination were analyzed using the Monte Carlo method, with consideration given to the number of columns $n$ ($n$ = 4, 6, 8, and 10) and the horizontal load coefficient $\gamma$ ($\gamma$ = 0.02, 0.04, 0.06, 0.08, and 0.1). Similarly, 20 groups of $F/P$ ratios were identified, and 20 groups of $F/P$ ratio probability density figures are shown in Figure 9.

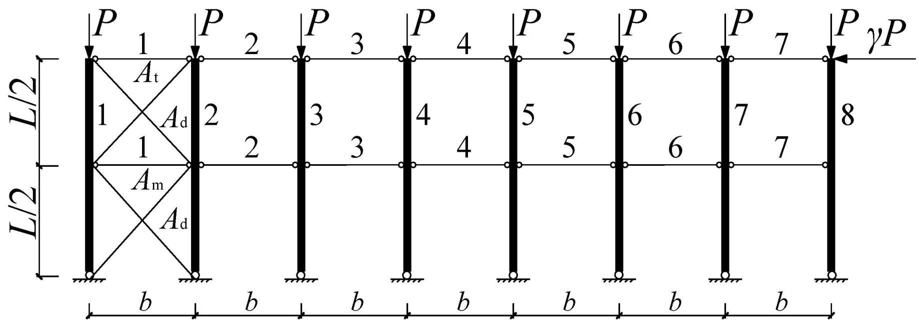


**Figure 8.** The analytical model under the most unfavorable horizontal load combination.

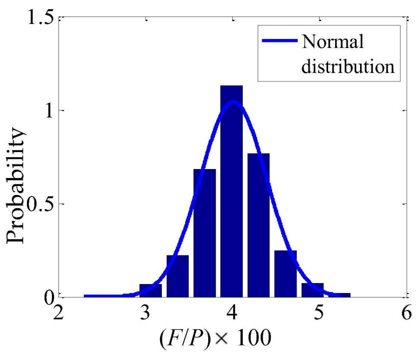


(**a**)

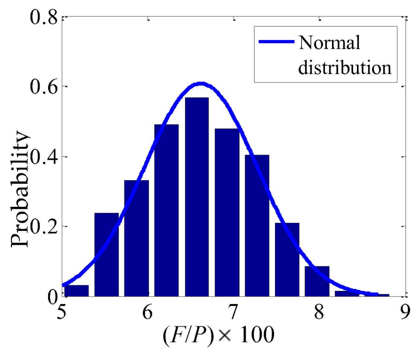


(**b**)

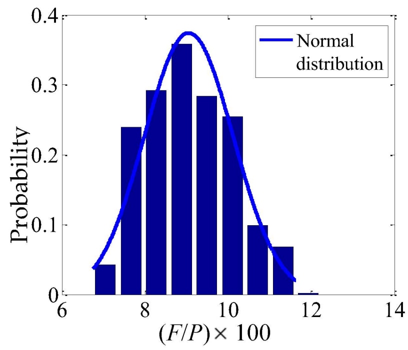


(**c**)

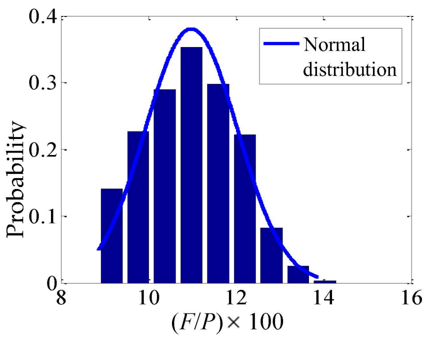


(**d**)

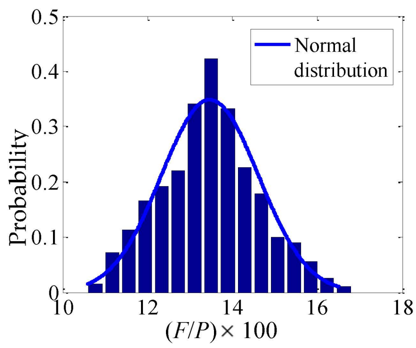


(**e**)

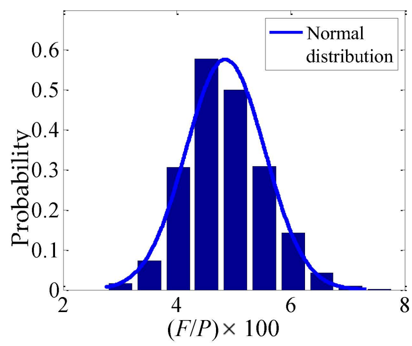


(**f**)

**Figure 9.** *Cont.*

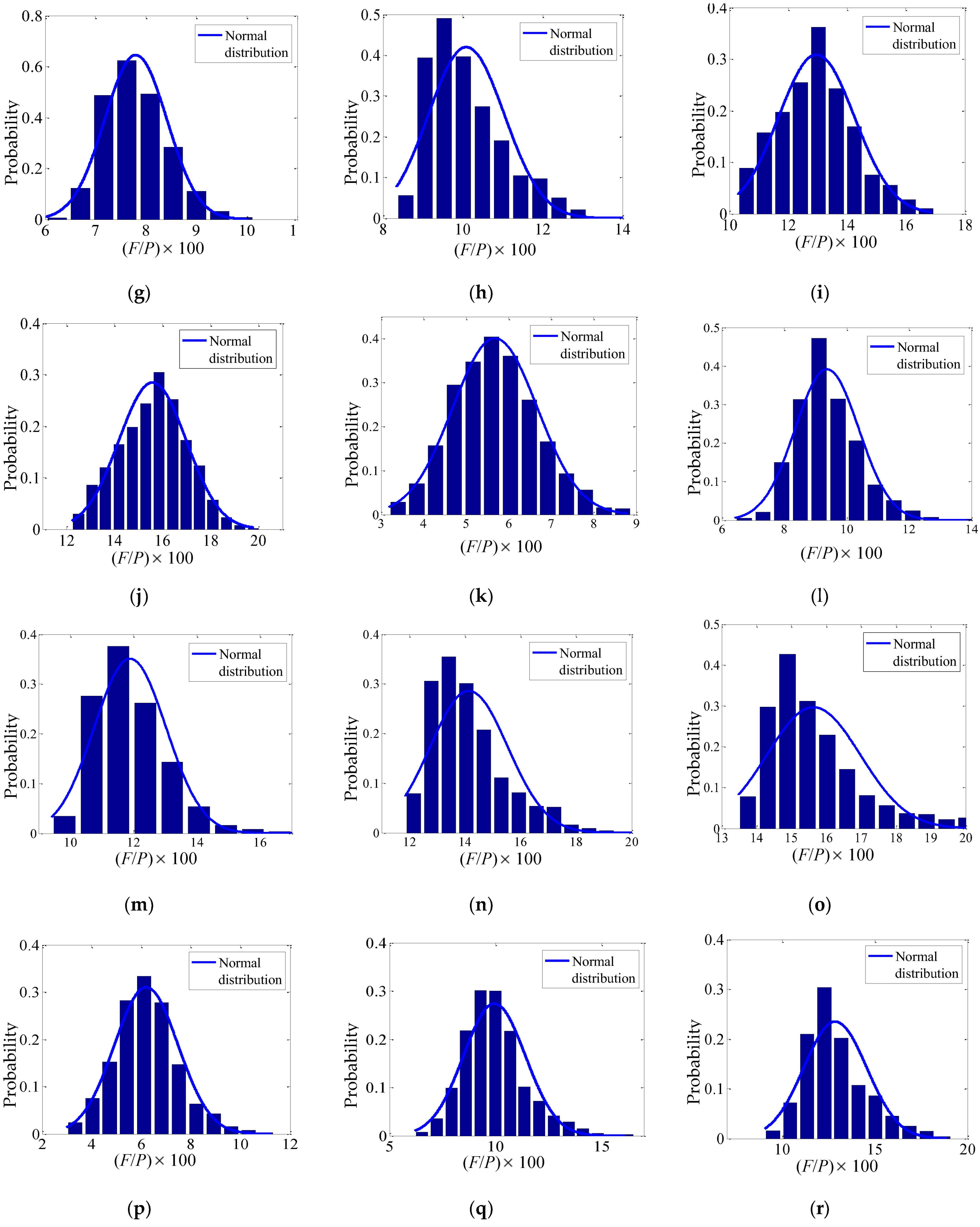


**Figure 9.** *Cont.*

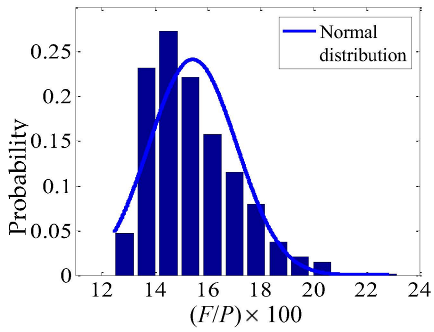


(**s**)

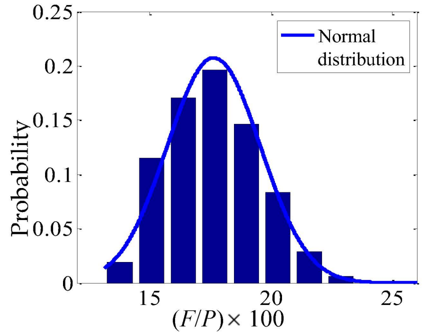


(**t**)

**Figure 9.** Probability density figures for F/P under the most unfavorable horizontal load combination. (**a**) $n = 4$ and $\gamma = 0.02$; (**b**) $n = 4$ and $\gamma = 0.04$; (**c**) $n = 4$ and $\gamma = 0.06$; (**d**) $n = 4$ and $\gamma = 0.08$; (**e**) $n = 4$ and $\gamma = 0.1$; (**f**) $n = 6$ and $\gamma = 0.02$; (**g**) $n = 6$ and $\gamma = 0.04$; (**h**) $n = 6$ and $\gamma = 0.06$; (**i**) $n = 6$ and $\gamma = 0.08$; (**j**) $n = 6$ and $\gamma = 0.1$; (**k**) $n = 8$ and $\gamma = 0.02$; (**l**) $n = 8$ and $\gamma = 0.04$; (**m**) $n = 8$ and $\gamma = 0.06$; (**n**) $n = 8$ and $\gamma = 0.08$; (**o**) $n = 8$ and $\gamma = 0.1$; (**p**) $n = 10$ and $\gamma = 0.02$; (**q**) $n = 10$ and $\gamma = 0.04$; (**r**) $n = 10$ and $\gamma = 0.06$; (**s**) $n = 10$ and $\gamma = 0.08$; (**t**) $n = 10$ and $\gamma = 0.1$.

### *6.2. Equations of Design Intermediate-height Horizontal Brace Forces*

Table 5 displays $F_n/P$ and $1.2{\times}F_n/P$ under the most unfavorable horizontal load combination. Furthermore, according to the number of columns $n$ and the horizontal load coefficient $\gamma$, $1.2 \times F_n/P$ can be given as follows:

**Table 5.** Statistical results of $(F/P) \times 100$ and $F_n/P$* under the most unfavorable horizontal load combination.

| $n$ | Horizontal Load Coefficient $\gamma$ | Statistical Character | $F_n/P$ | $1.2 \times F_n/P$ |
|---|---|---|---|---|
| 4 | 0.02 | $\mu = 4.0113$; $\sigma = 0.3830$ | 4.92% | 5.90% |
| | 0.04 | $\mu = 6.6207$; $\sigma = 0.6571$ | 7.94% | 9.53% |
| | 0.06 | $\mu = 8.4798$; $\sigma = 0.9039$ | 10.48% | 12.58% |
| | 0.08 | $\mu = 10.8835$; $\sigma = 0.9929$ | 13.45% | 16.14% |
| | 0.1 | $\mu = 13.4693$; $\sigma = 1.1447$ | 15.31% | 18.37% |
| 6 | 0.02 | $\mu = 4.8525$; $\sigma = 0.692$ | 5.99% | 7.19% |
| | 0.04 | $\mu = 7.7989$; $\sigma = 0.6184$ | 8.82% | 10.58% |
| | 0.06 | $\mu = 10.0892$; $\sigma = 0.9500$ | 11.99% | 14.39% |
| | 0.08 | $\mu = 12.3699$; $\sigma = 1.4123$ | 15.40% | 18.48% |
| | 0.1 | $\mu = 15.5835$; $\sigma = 1.4011$ | 17.88% | 21.46% |
| 8 | 0.02 | $\mu = 6.0589$; $\sigma = 0.9944$ | 7.89% | 9.47% |
| | 0.04 | $\mu = 9.3664$; $\sigma = 1.0182$ | 11.04% | 13.24% |
| | 0.06 | $\mu = 11.888$; $\sigma = 1.1361$ | 13.76% | 16.51% |
| | 0.08 | $\mu = 14.141$; $\sigma = 1.3949$ | 16.47% | 19.76% |
| | 0.1 | $\mu = 16.3568$; $\sigma = 1.6762$ | 19.16% | 22.99% |
| 10 | 0.02 | $\mu = 7.7995$; $\sigma = 1.2853$ | 9.98% | 11.98% |
| | 0.04 | $\mu = 9.9542$; $\sigma = 1.4562$ | 12.35% | 14.82% |
| | 0.06 | $\mu = 12.8625$; $\sigma = 1.6991$ | 15.67% | 18.80% |
| | 0.08 | $\mu = 15.4395$; $\sigma = 1.6526$ | 18.18% | 21.82% |
| | 0.1 | $\mu = 17.6446$; $\sigma = 1.9234$ | 20.82% | 24.98% |

The equations for design intermediate-height horizontal brace forces were obtained by a curve-fitting method from the FE analysis results summarized in Table 5, which are shown as follows.

$$\text{For } n = 4, \frac{F_n}{P} = 155\gamma + 3.02 \tag{11}$$

$$\text{For } n = 6,\ \frac{F_n}{P} = 160\gamma + 5.10 \tag{12}$$

$$\text{For } n = 8,\ \frac{F_n}{P} = 155\gamma + 7.26 \tag{13}$$

$$\text{For } n = 10,\ \frac{F_\text{n}}{P} = 150\gamma + 9.72 \tag{14}$$

where $\gamma$ is the horizontal load coefficient and the application range of equations for design intermediate-height horizontal brace forces is such that the value of $\gamma$ is not more than 0.1. In some cases, such as earthquake load, the horizontal load will be more than 0.1 $P$, which is beyond the research scope of this paper. An extensive parametric study would be conducted, and new equations would be proposed based on the extensive parametric study data in a separate paper, but this will be done in the future. The results listed in Table 5 are compared with Equations (11)–(14), as illustrated in Figure 10. This indicates that the design horizontal brace forces could be accurately and safely calculated by Equations (11)–(14) under different horizontal load coefficients. When $\lambda_\text{c}$ is larger, $P$ much depends on the stability, so a larger $F$ is required to ensure the stability of the column, and vice versa. In this paper, it is worth pointing out that the whole slenderness ratio of the column about the weak axis $2\lambda_\text{c}$ = 200 was adopted. As a result of $2\lambda_\text{c} \leq 150$ is used in most cases in engineering practice, the intermediate-height horizontal brace forces are less than those obtained in this paper. It is suggested that Equations (11)–(14) may be safely used in practice for column-braced systems under horizontal and vertical loads.

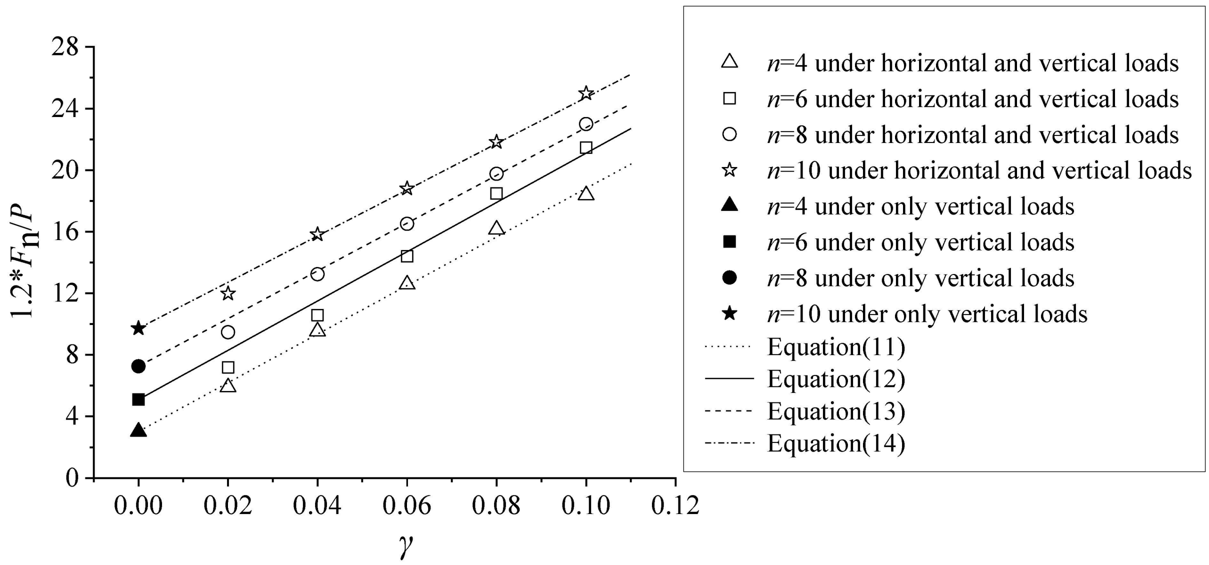


**Figure 10.** Variation in $1.2 \times F_\text{n}/P$ against $\gamma$.

## 7. Comparison with the Condition under Only Vertical Loads

Both Table 6 and Figure 10 show a comparison of $1.2 \times F_\text{n}/P$ between horizontal and vertical loads ($\gamma$ = 0.02 − 0.1) and only vertical loads ($\gamma$ = 0) [6]. It can be seen that $1.2 \times F_\text{n}/P$ under horizontal and vertical loads is much larger than $1.2 \times F_\text{n}/P$ under only vertical loads when $n$ is certain, and that $1.2 \times F_\text{n}/P$ under vertical and horizontal loads increases with an increase in the horizontal load coefficient $\gamma$ from 0.02 to 0.1. The reasons are the following: the horizontal loads decrease $P$ and the lateral stiffness of the columns, which can result in an increase in $F$ for σ, ensuring the longitudinal stability of columns.

The simple superposition results for the horizontal load coefficient $\gamma$ and $1.2 \times F_\text{n}/P$ ($\gamma$ = 0) under only vertical loads are shown in Table 6. It is shown that $1.2 \times F_\text{n}/P$ under horizontal and vertical loads is also larger than the simple superposition result $\gamma + 1.2 \times F_\text{n}/P$ ($\gamma$ = 0), and the reasons are the following: the horizontal loads amplify the $P - \Delta$ second-order effect and decrease the effective stiffness of intermediate-height horizontal braces, resulting in an increase in the intermediate-height horizontal brace force.

**Table 6.** Comparison of $1.2 \times F_n/P$ under horizontal and vertical loads with that under only vertical loads.

| *n* | $\gamma$ | $1.2 \times F_n/P$ | $\gamma + 1.2 \times F_n/P$ ($\gamma = 0$) |
|---|---|---|---|
| 4 | 0 | 3.02% | — |
| | 0.02 | 5.90% | 5.02% |
| | 0.04 | 9.53% | 7.02% |
| | 0.06 | 12.58% | 9.02% |
| | 0.08 | 16.14% | 11.02% |
| | 0.1 | 18.37% | 13.02% |
| 6 | 0 | 5.10% | — |
| | 0.02 | 7.19% | 7.10% |
| | 0.04 | 10.58% | 9.10% |
| | 0.06 | 14.39% | 11.10% |
| | 0.08 | 18.48% | 13.10% |
| | 0.1 | 21.46% | 15.10% |
| 8 | 0 | 7.26% | — |
| | 0.02 | 9.47% | 9.26% |
| | 0.04 | 13.24% | 11.26% |
| | 0.06 | 16.51% | 13.26% |
| | 0.08 | 19.76% | 15.26% |
| | 0.1 | 22.99% | 17.26% |
| 10 | 0 | 9.72% | — |
| | 0.02 | 11.98% | 11.72% |
| | 0.04 | 14.82% | 13.72% |
| | 0.06 | 18.80% | 15.72% |
| | 0.08 | 21.82% | 17.72% |
| | 0.1 | 24.98% | 19.72% |

## 8. Conclusions

The design horizontal brace forces under horizontal and vertical loads were derived using the Monte Carlo method, FE analysis, and probability model statistics, which accounted for initial imperfections with randomness in the horizontal braces and columns. The following is a summary of the conclusions:

(1) The normal probability density equation for intermediate-height horizontal brace forces under horizontal and vertical loads was proposed, and practical equations for design intermediate-height horizontal brace forces under horizontal and vertical loads were also developed, and it was determined that the design brace forces under vertical and horizontal loads are significantly greater than those under vertical loads alone.

(2) The intermediate-height horizontal brace forces under horizontal and vertical loads are also much larger than the simple superposition results for the horizontal load coefficient $\gamma$ and the intermediate-height horizontal brace forces under only vertical loads, because the horizontal loads amplify the $P - \Delta$ second-order effect and decrease the effective stiffness of intermediate-height horizontal braces.

(3) The whole slenderness ratio of the column about the weak axis $2\lambda_c = 200$ is conservatively adopted. This is mainly because the intermediate-height horizontal brace force increases with an increase in $\lambda_c$. As a result of $2\lambda_c \leq 150$ is used in most cases of practical design, the intermediate-height horizontal brace forces in engineering practice are much less than those proposed in this study.

**Author Contributions:** Conceptualization, J.Z. and H.Y.; methodology, J.Z. and H.Y.; software, J.Z. and S.L.; validation, J.Z. and S.L.; formal analysis, J.Z. and S.L.; investigation, J.Z. and H.Y.; resources, S.L.; data curation, J.Z. and H.Y.; writing—original draft preparation, H.Y. and S.L.; writing—review and editing, J.Z., H.Y., Z.F. and S.L.; visualization, S.L.; supervision, J.Z., H.Y. and Z.F.; project administration, J.Z. All authors have read and agreed to the published version of the manuscript.

**Funding:** This research was funded by the National Natural Science Foundation of China, grant number: 51008055 and the Natural Science Foundation of Heilongjiang Province, grant number: E2015056.

**Data Availability Statement:** Not applicable.

**Conflicts of Interest:** The authors declare no conflict of interest. The funders had no role in the design of the study; in the collection, analyses, or interpretation of data; in the writing of the manuscript; or in the decision to publish the results.

## References

1. Winter, G. Lateral bracing of columns and beams. *J. Struct. Div. ASCE* **1958**, *84*, 1–22. [CrossRef]
2. Yura, J.A. Winter's bracing approach revised. *Eng. Struct.* **1996**, *18*, 821–825. [CrossRef]
3. Tong, G.S.; Chen, S.P. Design requirement for bracing between columns. *Ind. Constr.* **2003**, *33*, 9–12. (In Chinese)
4. Li, D. *Stability Analysis and Bracing Requirements of Longitudinal Braced Frames*; Zhejiang University: Hangzhou, China, 2005.
5. Zhang, Y.C.; Zhao, J.Y.; Zhang, W.Y. Parametric Studies on Inter-column Brace Forces. *Adv. Struct. Eng.* **2008**, *11*, 305–315. [CrossRef]
6. Zhao, J.Y.; Zhang, Y.C.; Lin, Y.Y. Study on mid-height horizontal bracing forces considering random initial geometric imperfections. *J. Constr. Steel Res.* **2014**, *92*, 55–66. [CrossRef]
7. Chen, B.; Roy, K.; Uzzaman, A.; Raftery, G.M.; Nash, D.; Clifton, G.C.; Pouladi, P.; Lim, J.B.P. Effects of edge-stiffened web openings on the behaviour of cold-formed steel channel sections under compression. *Thin-Walled Struct.* **2019**, *144*, 106307. [CrossRef]
8. Klasson, A.; Crocetti, R.; Hansson, E.F. Slender steel columns: How they are affected by imperfections and bracing stiffness. *Structures* **2016**, *8*, 35–43. [CrossRef]
9. Kala, Z. Geometrically non-linear finite element reliability analysis of steel plane frames with initial imperfections. *J. Civil Eng. Manag.* **2012**, *18*, 81–90. [CrossRef]
10. Sheidaii, M.R.; Gordini, M. Effect of Random Distribution of Member Length Imperfection on Collapse Behavior and Reliability of Flat Double-Layer Grid Space Structures. *Adv. Struct. Eng.* **2015**, *18*, 1475–1485. [CrossRef]
11. Chen, B.; Roy, K.; Fang, Z.; Uzzaman, A.; Raftery, G.M.; Lim, J.B.P. Moment capacity of back-to-back cold-formed steel channels with edge -stiffened hole, un-stiffened hole, and plain web. *Eng. Struct.* **2021**, *235*, 112042. [CrossRef]
12. Zhang, X.L.; Xue, J.Y.; Han, Y.; Chen, S.L. Model test study on horizontal bearing behavior of pile under existing vertical load. *Soil Dyn. Earthq. Eng.* **2021**, *147*, 106820.
13. Dou, C.; Pi, Y.L. Effects of Geometric Imperfections on Flexural Buckling Resistance of Laterally Braced Columns. *J. Struct. Eng.* **2016**, *142*, 04016048. [CrossRef]
14. Czepiżak, D.; Biegus, A. Refined calculation of lateral bracing systems due to global geometrical imperfections. *J. Constr. Steel Res.* **2016**, *119*, 30–38. [CrossRef]
15. Klasson, A.; Crocetti, R.; Björnsson, I.; Hansson, E.F. Design for lateral stability of slender timber beams considering slip in the lateral bracing system. *Structures* **2018**, *16*, 157–163. [CrossRef]
16. ANSYS Inc., ANSYS Mechanical APDL Structural Analysis Guide: ANSYS Release 13.0, USA, 2010. Available online: https://www.mm.bme.hu/~{}gyebro/files/fea/ansys/ansys_13_element_reference.pdf (accessed on 3 January 2023).
17. Zhao, J.Y. *Bracing Design Method of Longitudinal Column-Bracing System Under Vertical Loading*; Harbin Institute of Technology: Harbin, China, 2009. (In Chinese)
18. Xu, Z.J. *Monte Carlo Method*; Shanghai Technology and Science Publishing House: Shanghai, China, 1985.
19. Nowak, A.S.; Collins, K.R. *Reliability of Structures*; The McGraw-Hill Education (Asia) Companies Press: Boston, MA, USA, 2000.
20. Zhang, Y.C.; Jin, L.; Shao, Y.S. Practical advanced design considering random distribution of initial geometric imperfections. *Adv. Struct. Eng.* **2011**, *14*, 379–389. [CrossRef]
21. Tong, G.S.; Chen, S.F. Design forces of horizontal inter-column braces. *J. Constr. Steel Res.* **1987**, *75*, 363–370. [CrossRef]
22. Zhao, J.Y.; Wei, J.M.; Wang, J. Design forces of horizontal braces unlocated at middle of columns considering random initial geometric imperfections. *Adv. Civil Eng.* **2021**, *2021*, 1264270. [CrossRef]
23. Wei, J.P.; Tian, L.M.; Hao, J.P.; Li, W.; Zhang, C.B.; Li, L.J. Novel principle for improving performance of steel frame structures in column-loss scenario. *J. Constr. Steel Res.* **2019**, *163*, 105768. [CrossRef]
24. Chen, B.; Roy, K.; Uzzaman, A.; Raftery, G.M.; Lim, J.B.P. Moment capacity of cold-formed channel beams with edge-stiffened web holes, un-stiffened web holes and plain webs. *Thin-Walled Struct.* **2020**, *157*, 107070. [CrossRef]
25. Piątkowski, M. Experimental research on load of transversal roof bracing due to geometrical imperfections of truss. *Eng. Struct.* **2021**, *242*, 112558. [CrossRef]
26. Wang, L.; Helwig, T.A. Critical Imperfections for Beam Bracing Systems. *J. Struct. Eng.* **2005**, *131*, 933–940. [CrossRef]
27. *GB50205*; Code for acceptance of construction quality of steel structures. Chinese Planning Press: Beijing, China, 2001.

28. O'Reilly, G.J.; Goggins, J. Experimental testing of a self-centring concentrically braced steel frame. *Eng. Struct.* **2021**, *238*, 111521. [CrossRef]
29. Meng, B.; Zhong, W.H.; Hao, J.P.; Song, X.Y. Improving anti-collapse performance of steel frame with RBS connection. *J. Constr. Steel Res.* **2020**, *170*, 106119. [CrossRef]
30. Shen, P.W.; Yang, P.; Hong, J.H.; Yang, Y.M.; Tuo, X.Y. Seismic performance of steel frame with a self-centering beam. *J. Constr. Steel Res.* **2020**, *175*, 106349. [CrossRef]